XVIII. Polymer Research

PROPULSION DIVISION

A. Viscoelastic Behavior of Elastomers Undergoing Crosslinking Reactions,

J. Moacanin and J. J. Aklonis[1]

Previously (SPS 37-54, -57, -58, -59, -61, and -63, Vol. III) a framework was developed for the prediction of the physical behavior of polymers which are reacting while being subjected to stress relaxation, creep, or dynamic relaxation experiments. These predictions, however, were made for systems where scission was the only chemical reaction taking place. Here we extend the previous results to the prediction for systems where creep or stress relaxation experiments are conducted while crosslinking reactions are occurring. Since this situation is considerably more complicated than is the case of the scission reaction, we will deal only with a single instantaneous change in crosslink density $\nu_1 \rightarrow \nu_2$, where $\nu_2 > \nu_1$. Calculations will be made to allow prediction of behavior for this single transition system; equations for cases where the crosslinking reaction is continuous will be derived but will not be solved.

Consider a creep experiment on a sample with crosslink density ν_1 subjected to a stress σ. At any time, the length of this sample may be given as

$$L(t) = [1 + \epsilon(t)]\, L_0 = [1 + D_{\nu_1}(t)\sigma]L_0 \qquad (1)$$

At t^*, the change ν_1 to ν_2 is effected at virtually constant length and the behavior of the system at $t > t^*$ will depend on $D_{\nu_2}(t)$ and no longer on $D_{\nu_1}(t)$. The plausibility of this basic assumption has been argued previously (SPS 37-59, Vol. III).

Therefore, at times greater than t^* all of the relaxation mechanisms are governed by the character of a ν_2 network. But the chains are of two types. The fraction ν_1/ν_2 of all the chains is supporting stress at t^*, whereas the fraction $(\nu_2 - \nu_1)/\nu_2$ is not. The latter fraction represents the new chains which are always relaxed when formed (Ref. 1). Proceeding to introduce $\bar{m}$ by equating

[1]Department of Chemistry, University of Southern California, Los Angeles, California.

sample length before and after the crosslink density change at t^*, we get

$$L(t^*) = [1 + D_{\nu_1}(t^*)\sigma]L_0 = \left[1 + \left(\frac{\nu_2}{\nu_1}\right)D_{\nu_2}(t^* + \bar{m})\,\sigma\right]L_0 \tag{2}$$

Here the factor ν_2/ν_1 accounts for the fact that only a fraction of the chains of character ν_2 are supporting stress at t^*. Rearrangement of Eq. (2) yields

$$D_{\nu_1}(t^*) = \frac{\nu_2}{\nu_1} D_{\nu_2}(t^* + \bar{m}) \tag{3}$$

which defines the time shift $\bar{m}$ in terms of ν_1, ν_2 and the corresponding compliance functions.

As the sample creep continues at $t > t^*$, the stress σ gradually shifts from the original ν_1/ν_2 fraction of chains to the newly added chains. Therefore the distribution of the total stress σ between the two fractions of the network must be described.

According to the Boltzmann Superposition Principle (Ref. 1), the time-dependent strain $\epsilon(t)$, which results from any time-dependent stress $\sigma(t)$ applied to a system whose compliance $D(t)$ is known, may be calculated according to the equation

$$\epsilon(t) = \int_0^t \dot{\sigma}(\tau)D(t - \tau)\,d\tau \tag{4}$$

For times greater than t^*, the strain $\epsilon_1(t)$ on the ν_1/ν_2 chains now at crosslink density ν_2 may be given as

$$\epsilon_1(t) = \sigma\frac{\nu_2}{\nu_1} D_{\nu_2}(t + \bar{m}) + \int_{t^*}^t \dot{\sigma}_1(\tau)\frac{\nu_2}{\nu_1} D_{\nu_2}(t - \tau)\,d\tau \tag{5}$$

The first term on the right-hand side describes the response of the ν_1/ν_2 chains subjected to the total stress σ, and the second term accounts for the stress transfer between the two networks.

Similarly for the $(\nu_2 - \nu_1)/\nu_2$ newly formed chains, the strain $\epsilon_2(t)$ for times greater than t^* would be given as

$$\epsilon_2(t) = \int_{t^*}^t \dot{\sigma}_2(\tau)\frac{\nu_2}{\nu_2 - \nu_1} D_{\nu_2}(t - \tau)\,d\tau \tag{6}$$

For a creep experiment, however, the total stress is constant; hence,

$$\left.\begin{aligned} \sigma &= \sigma_1 + \sigma_2 \\ \text{or} \qquad \dot{\sigma}_1 &= -\dot{\sigma}_2 \end{aligned}\right\} \tag{7}$$

and Eq. (6) becomes

$$\epsilon_2(t) = -\int_{t^*}^t \dot{\sigma}_1(\tau)\frac{\nu_2}{\nu_2 - \nu_1} D_{\nu_2}(t - \tau)\,d\tau \tag{8}$$

Additional constraints are imposed by the fact that both networks are part of the same macroscopic system; accordingly, for times greater than t^*, the definitions depicted in Fig. 1 show that

$$D_1(t) = \frac{\Delta L^* + \Delta L(t)}{L_0} \tag{9}$$

For the $(\nu_2 - \nu_1)/\nu_2$ new chains which are relaxed at t^*, however, the unstretched length which should appear in the denominator is $L_0 + \Delta L^*$. Accordingly, we define

$$D_2(t) = \frac{\Delta L(t)}{L_0 + \Delta L^*} \tag{10}$$

Elimination of $\Delta L(t)$ from Eqs. (9) and (10) yields the relationship

$$L_0\epsilon_1(t) - \Delta L^* = \epsilon_2(t)(L_0 + \Delta L^*) \tag{11}$$

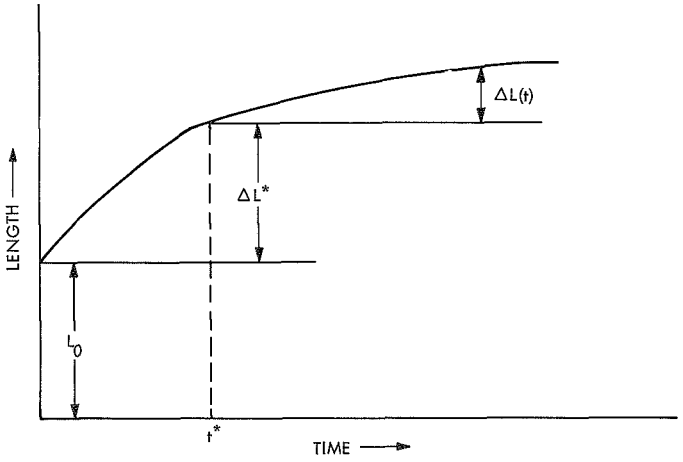

Fig. 1. Creep of an elastomer with a single crosslinking step at t^*

Substitutions of Eqs. (5) and (8) into Eq. (11) yield

$$\int_{t^*}^{t} \dot{\sigma}(\tau) D_{\nu_2}(t-\tau)\, d\tau = \frac{\Delta L^* - L_0 \sigma_T \frac{\nu_2}{\nu_1} D_{\nu_2}(t+\bar{m})}{L_0 \frac{\nu_2}{\nu_1} + L_0 \frac{\nu_2}{\nu_2 - \nu_1} + \Delta L^* \frac{\nu_2}{\nu_2 - \nu_1}} \tag{12}$$

In principle Eq. (12) may be solved for $\dot{\sigma}(t > t^*)$; this function may then be used for $\dot{\sigma}_1(\tau)$ in Eq. (5) to calculate $\epsilon_1(t)$, which can then be related to the length of the total sample as a function of time. To make the algebra tractable for computer calculations, we have generated from Eq. (12) recursion relationships in terms of finite differences. Parametric calculations are in progress.

Reference

1. Tobolsky, A. V., "Properties and Structure of Polymers," Chap. 3. John Wiley & Sons, Inc., New York, 1960.

B. Energy Transfer in Bipyridilium (Paraquat) Salts, *A. Rembaum, V. Hadek, and S. P. S. Yen*

The high electron affinity of 4,4′-bipyridilium (paraquat) salts, well-known herbicides (Ref. 1), has been demonstrated in 1933 by Michaelis and Hill (Ref. 2) who have shown that bipyridilium bases can be reduced to form colored species. The colorless bivalent cation accepts an electron to form II, a violet univalent cation, and this process may be represented by the following equilibrium:

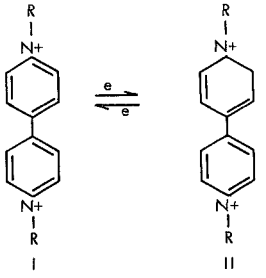

where R is generally an aryl or alkyl group or a hydrogen atom.

II has several resonating structures and this fact is responsible for the absorption maximum in the long wavelength range of the spectrum (between 5700 to 6000 Å, depending on the structure of R).

The ease of reduction of paraquat is attributed to its high electron affinity which is also responsible for the formation of a variety of charge transfer complexes between paraquats and phenols, quinones, hydroquinones, etc. (Refs. 3–5), the latter acting as electron donors and the paraquats as electron acceptors.

We report a charge transfer interaction between paraquat and 8,8,8′8′-tetracyanoquinodimethane radical anion ($TCNQ^{\cdot-}$). The purpose of our investigation was to determine whether an electron transfer occurs from $TCNQ^{\cdot-}$ to structure I and to compare the electron transport properties of aliphatic with aromatic tetracyanoquinodimethane salts. We have found that:

(1) The paraquat salt I in which R = H when reacted with 2 molecules of $LiTCNQ^{\cdot-}$ exhibits a surprisingly low electrical resistivity (about 1 to 10 Ω-cm) and that on addition of neutral TCNQ the electrical resistivity remains unaltered. Furthermore, the same salt with $R = CH_3$ formed under identical conditions is characterized by a resistivity of the order of 10^6 Ω-cm. However, the addition of neutral TCNQ to the latter reduces the electrical resistivity by about five orders of magnitude.

(2) The visible spectra of the aliphatic diammonium and bipyridilium TCNQ salts exhibited the characteristic features previously reported for a number of other TCNQ compounds (Refs. 6 and 7).

(3) The electronic transport properties of aliphatic diammonium TCNQ salts do not differ significantly from the corresponding bipyridilium salts,

Table 1. Aliphatic diammonium TCNQ salts

Diammonium salt	Ratio used in synthesis					
	1 mole diammonium salt:2 moles $Li^+TCNQ^{\cdot-}$			1 mole diammonium salt:2 moles $Li^+TCNQ^{\cdot-}$: 2 moles $TCNQ^0$		
	Resistivity ρ, Ω-cm	Activation energy ϵ, eV	Seebeck coefficient α, $\mu V/°C$	Resistivity ρ, Ω-cm	Activation energy ϵ, eV	Seebeck coefficient α, $\mu V/°C$
$(CH_3)_2N(CH_2)_5N(CH_3)_2$, 2HBr	4.0×10^6	0.29	+410	1.2×10^2	0.22	−150
$(CH_3)_2N(CH_2)_6N(CH_3)_2$, 2HI	5.0×10^{10}	0.73	—	1.0×10^2	0.21	−143
$(CH_3)_2N(CH_2)_8N(CH_3)_2$, 2HBr	3.7×10^7	0.41	+720	7.0	0.090	−10

Table 2. Bipyridilium TCNQ salts

Bipyridilium salt reference No.	Ratio used in synthesis					
	1 mole BP salt:2 moles $Li^+TCNQ^{\cdot-}$			1 mole BP salt:2 moles $Li^+TCNQ^{\cdot-}$:2 moles $TCNQ^0$		
	Resistivity ρ, Ω-cm	Activation energy ϵ, eV	Seebeck coefficient α, $\mu V/°C$	Resistivity ρ, Ω-cm	Activation energy ϵ, eV	Seebeck coefficient α, $\mu V/°C$
4,4′-BP,2HCl	1.5	0.090	−66	1.2	0.098	−65
2,2′-BP,2HCl	1.4	0.060	−56	1.0	0.058	−52
4,4′-BP,2HI	12.0	0.110	−65	9.0	0.103	−66
4,4′-BP,2CH_3I	1.1×10^6	0.65	+150	22.0	0.130	−37

with the exception of the case where electron transfer occurs (when R = H).

The electronic transport properties of aliphatic diammonium compounds and bipyridilium TCNQ salts are shown in Tables 1 and 2, respectively. The investigated samples were prepared by reacting one mole of the diammonium salt in the form of dichloride or diiodide with two moles of $LiTCNQ^{\cdot-}$. Another series of samples was prepared by reacting the above diammonium salts with two moles of $LiTCNQ^{\cdot-}$ and two moles of neutral TCNQ (referred to as $TCNQ^0$).

Table 1 confirms the previous results (Ref. 7), namely, the electrical resistivity of diammonium TCNQ salts in which both positive nitrogens are associated with a $TCNQ^{\cdot-}$ is five to six orders of magnitude higher than the resistivity of the same compounds containing, in addition to the radical ion ($TCNQ^{\cdot-}$), a neutral TCNQ molecule.

Table 2 illustrates the same facts for N,N′ dimethyl-4,4′-bipyridilium TCNQ compound (4,4′-BP,2CH_3I). However, the N,N′-dihydro-4,4′ and 2,2′-bipyridilium TCNQ salts (4,4′-BP,2HCl, and 2,2′-BP,2HCl) constitute exceptions of what appeared to be a general rule. This anomalous behavior was elucidated by examination of the absorption spectra in the visible range in conjunction with the electrical properties.

A calibration curve (Fig. 1) was determined using synthetic mixtures of $LiTCNQ^{\cdot-}$ and $TCNQ^0$. The plot of the intensity ratio of λ_{max} at 3950 Å to 8420 Å versus the ratio of $TCNQ^{\cdot-}$:$TCNQ^0$ served to estimate the composition of TCNQ salts and compare the latter with the electrical resistivity (Table 3).

On the basis of the above results it is possible to conclude that electron transfer occurs from $TCNQ^{\cdot-}$ in structure III to yield structure IV, while in the case where a CH_3 group is bonded to the positive nitrogen no electron transfer is observed.

The electron transfer results in the oxidation of $TCNQ^{\cdot-}$ to $TCNQ^0$ and is therefore responsible for the low

Table 3. Correlation of resistivity with the ratio $TCNQ^{\cdot-}$:$TCNQ^0$

Bipyridilium salt reference No.	Intensity ratio at $\frac{\lambda_{max}\ 3950\ Å}{\lambda_{max}\ 8420\ Å}$	Number of moles in BP salt		Resistivity ρ, Ω-cm
		$TCNQ^{\cdot-}$	$TCNQ^0$	
4,4′-BP,2HCl	2.25	1	1	1.5
2,2′-BP,2HCl	2.25	1	1	1.4
4,4′-BP,2HI	2.25	1	1	1.2×10
4,4′-BP,2CH_3I		2	0	1.1×10^6
4,4′-BP,2CH_3I	1.2	2	1	2.2×10

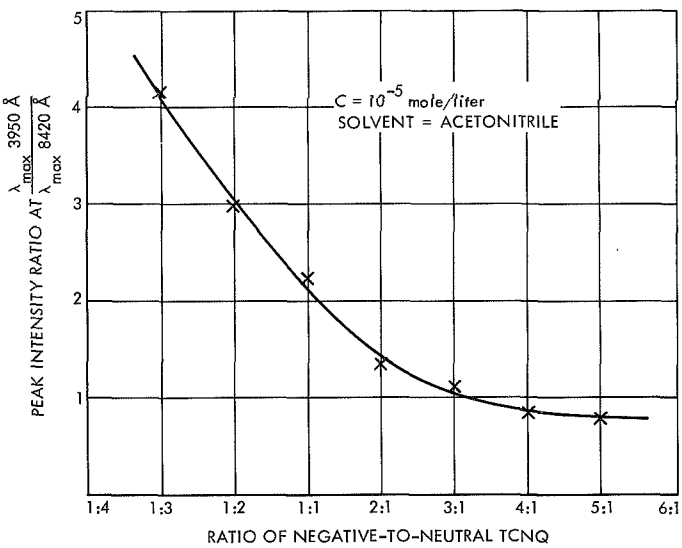

Fig. 1. Calibration curve to determine negative-to-neutral TCNQ ratio according to peak-height ratio of spectral bands 3950 Å and 8420 Å

resistivity of salts in which the positive nitrogen is bonded to a hydrogen. Thus, the reaction of structure I with LiTCNQ leads to a salt containing both the radical anion as well as a neutral TCNQ molecule; therefore its high electronic conductivity is not surprising. The formation of structure II in the electron transfer process does not appear likely on the basis of the observed absorption spectra (Ref. 2). The following mechanism is therefore proposed:

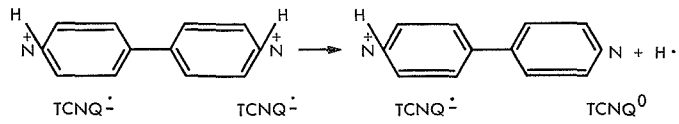

III IV

It is assumed that the hydrogen atom reacts with the solvent or dimerizes and the absence of an oxidation-reduction reaction in methyl-substituted species may be due to the inductive effect of the methyl group. Alternatively the N—CH_3 bond being stronger than the N—H bond, the splitting of the hydrogen atom in structure III could be explained on the basis of bond strength. This assumption appears more plausible since the oxidation reduction potentials of 4,4′-BP,CH_3I and 4,4′-BP,HCl determined polarographically were found to be practically identical, indicating the same electron affinity.

The increase in conductivity of salts containing $TCNQ^0$ is consistent with the theoretical derivations of LeBlanc (Ref. 8) who accounted for the high conductivity of the complex salts by hole–electron pairs in the Heitler London ground state configuration without placing two electrons on the same TCNQ site and therefore avoiding formation of a dianion. In this interpretation the presence of a neutral TCNQ molecule is necessary for efficient electron transport.

References

1. Boon, W. R., *Endeavour*, Vol. XXVI, p. 27, 1967.
2. Michaelis, L., and Hill, E. S., *J. Gen. Phys.*, Vol. 16, p. 859, 1933.
3. MacFarlane, A. J., and Williams, R. T. P., *J. Chem. Soc.*, Part A, p. 1517, 1969.
4. White, B. G., *Trans. Faraday Soc.*, Vol. 65, p. 2000, 1969.
5. Ledwith, A., and Woods, H. J., *J. Chem. Soc.*, p. 1422, 1970.
6. Melby, L. R., et al., *J. Amer. Chem. Soc.*, Vol. 84, p. 3374, 1962.
7. Rembaum, A., et al., *J. Phys. Chem.*, Vol. 73, p. 513, 1969.
8. LeBlanc, O. H., *J. Chem. Phys.*, Vol. 42, p. 4307, 1965.

C. Electrical Properties of TCNQ Salts of Ionene Polymers and Their Model Compounds,

V. Hadek, H. Noguchi, and A. Rembaum[1]

1. Introduction

The discovery of highly conductive 7,7′,8,8′-tetracyanoquinodimethane (TCNQ) paramagnetic salts constitutes an important advance in the study of electronic conductivity of purely organic materials. This high conductivity is exhibited by monosalts or polysalts, provided the TCNQ radical anion ($TCNQ^{\cdot}$) is associated with a neutral TCNQ molecule ($TCNQ^{0}$) (Refs. 1–3). Although the electronic conductivity of this type of material has already been well established (Ref. 4), no data are available as yet on the electrical properties of TCNQ polymers as a function of polymer structure.

The present investigation was undertaken in order to gain insight into the mechanism of electronic conductivity of polymeric TCNQ salts, formed from polyelectrolytes, the structure of which could be systematically altered. Ionene polymers (Ref. 5) of well-defined structure seemed to be ideally suited for this purpose. The latter was therefore synthesized by means of the following reaction:

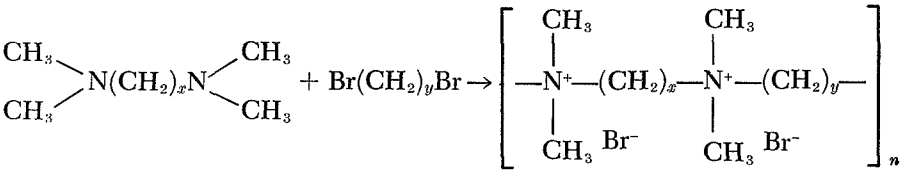

$x - y$ ionene bromide

(1)

where x and y are integers, and n is the number of unit segments. The kinetics of formation and some solution properties of these polymers were recently described (Ref. 6).

Electrically conducting polysalts were prepared by the reaction of x-y ionene bromides with LiTCNQ in presence or in absence of $TCNQ^{0}$. It was found that the specific resistivity and the activation energy for conduction of a 6-6 ($x = 6$ and $y = 6$) ionene polysalt was considerably higher than a number of similar polysalts with different x and y values. In order to elucidate this anomaly, a homologous series of model TCNQ compounds representing unit segments of the polymers was synthesized from polymethylene *bis*-(trimethylammonium halides) and their electrical properties were compared with those of TCNQ polysalts. The large variations in electrical properties were found to depend mainly on the geometrical configuration and crystal packing and not on the distances between positively charged nitrogen atoms in the polyelectrolytes.

2. Results

a. Ionene polymers. The first series of polymeric TCNQ salts was prepared by reacting ionene bromides (intrinsic viscosity $[\eta] = 0.154$ to 0.791 dl/g measured in 0.4 mole KBr aq. solution) with LiTCNQ, using a molar ratio of unit segment to LiTCNQ of 1.2. The intrinsic viscosity of the polymers, the yields, and chemical analyses are recorded in Table 1.

The second series of polysalts was prepared by reacting ionene bromides with a mixture of LiTCNQ and $TCNQ^{0}$ using a molar ratio of 1:2:2.

The electrical properties of the polysalts, i.e., resistivity (ρ), activation energy (ϵ), and Seebeck coefficient (α) in absence and in presence of $TCNQ^{0}$, are recorded in Table 2. The dramatic changes in resistivity of salts in which $x = 4$ or 6 and $y = 3$, 5, 6, 8, 10, and 16 are shown in Fig. 1.

[1]Acknowledgement made to the National Academy of Sciences, National Research Council, Washington, D. C., for the Postdoctoral Resident Associateships supporting this research, and to Dr. R. Bau, University of Southern California, for assistance in the x-ray investigations.

b. Model compounds (DiTCNQ salts). The model compounds, namely, polymethylene *bis*-(trimethylammonium halides), were prepared by means of reaction (2) or (3):

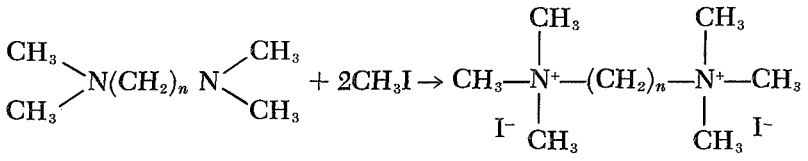

(2)

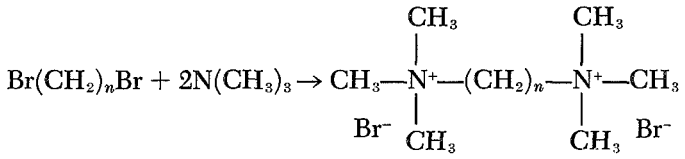

(3)

The details of synthesis and chemical analysis are shown in Table 3.

Table 1. Synthesis of TCNQ polysalts (in absence of TCNQ⁰)

x-y	[η], dl/g	Temperature, °C	Yield, %	Elemental composition						
				Calculated,[a] %			Found, %			
				C	H	N	C	H	N	Br
3-4	0.154	60–65	85.1	70.69	5.76	23.55	67.01	6.36	19.95	2.13
6-3	0.246	22–30	81.9							
6-3	0.246	60–65	84.7							
6-5	0.482	22–30	82.2							
6-5	0.482	60–65	91.9							
6-6	0.299	22–30	—							
6-6	0.299	60–65	96.1							
6-8	0.577	22–30	91.0							
6-8	0.577	60–65	97.5							
6-8	0.577	60–65	85.9	72.80	6.98	20.21	68.62	7.68	15.73	3.71
6-10	0.791	22–30	94.4							
6-10	0.791	60–65	90.3	73.30	7.27	19.43	70.23	7.90	15.70	3.23
6-16	0.157	22–30	51.6							
6-16	0.157	60–65	63.0	74.59	8.01	17.40	73.17	8.32	14.71	0.13

[a]Calculated for the idealized structure:

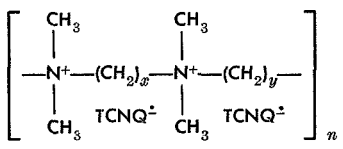

Table 2. Electrical properties of the TCNQ polysalts

Numbers of CH_2 group (x-y)	One-unit segment to $2TCNQ^{\cdot-}$			One-unit segment to $2TCNQ^{\cdot-}$ $2TCNQ^{0}$ with negative and neutral TCNQ		
	Resistivity ρ, Ω-cm	Activation energy ϵ, eV	Seebeck coefficient α, mV/°C	Resistivity ρ, Ω-cm	Activation energy ϵ, eV	Seebeck coefficient α, mV/°C
3-4	2.8×10^4	0.22	+0.12	1.5×10^3	0.20	+0.09
6-3	9.5×10^5	0.30	+0.31	3.4×10^3	0.24	+0.06
6-5	1.5×10^8	0.56	Positive[a]	7.7×10^1	0.140	−0.027
6-6	3.2×10^8	0.58	Positive[a]	5.2×10^7	0.46	+0.93
6-8	7.2×10^7	0.52	+0.72	1.4×10^7	0.45	+0.66
6-10	3.0×10^6	0.39	+0.39	7.3×10^4	0.29	+0.27
6-16	9.6×10^6	0.48	+0.04	4.7×10^2	0.23	−0.008

[a]The Seebeck coefficient was positive but its exact value could not be determined because of polarization effects.

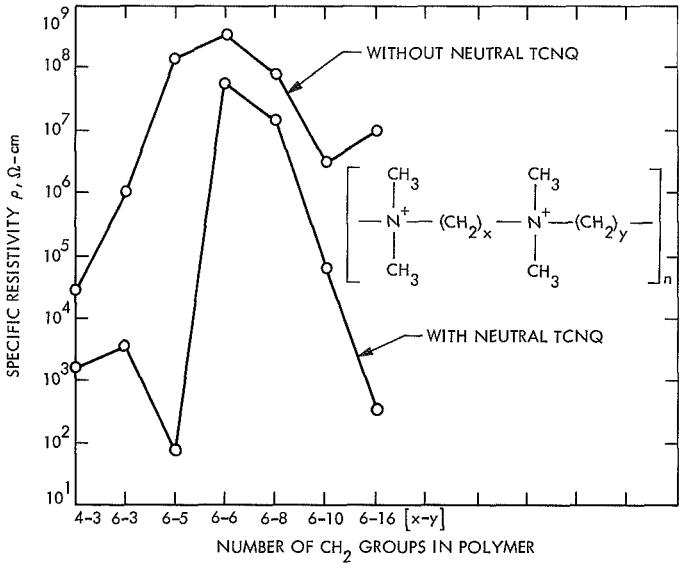
SPECIFIC RESISTIVITY ρ, Ω-cm
WITHOUT NEUTRAL TCNQ
WITH NEUTRAL TCNQ
4-3 6-3 6-5 6-6 6-8 6-10 6-16 [x-y]
NUMBER OF CH2 GROUPS IN POLYMER

Fig. 1. Specific resistivities of TCNQ salts derived from the model compounds as a function of the number of CH_2 groups

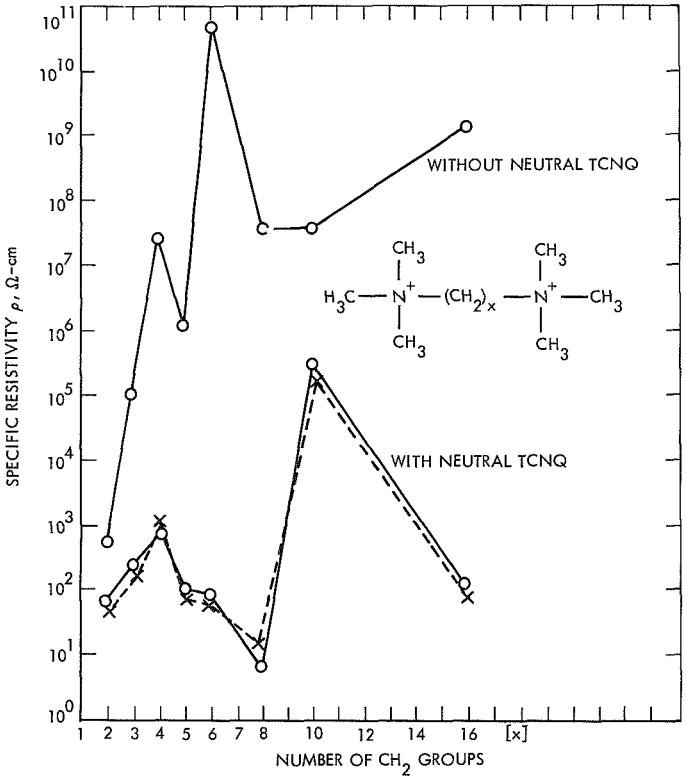

Fig. 2. Specific resistivities of TCNQ salts derived from ionene polymers as a function of the numbers of CH_2 groups

The model compounds were subsequently reacted with LiTCNQ and the obtained disalts had the composition $M^{2+}(TCNQ^{\cdot-})_2$, where M^{2+} represents the polymethylene *bis*-(trimethylammonium) dication, which is generally in excellent agreement with the chemical analysis (Table 4). Similarly, when the model compounds were reacted with LiTCNQ and $TCNQ^0$ using the three reagents in a molar ratio of 1:2:2, another series of disalts was obtained. The electrical properties of both types of model salts are recorded in Table 5 and the resistivity versus number of CH_2 groups is shown in Fig. 2. The resistivity values of the same batch of materials could be reproduced with an accuracy of ±10%.

The broken line (Fig. 2) represents the resistivity of salts prepared at 65°C and allowed to crystallize for

Table 3. Synthesis of polymethylene *bis*-(trimethylammonium halides)

n	Reaction	Concentration		Reaction time, h	Yield, %		Recrystallization solvent	Elemental composition								
								Calculated, %					Found, %			
					I[a]	II[b]		Type of halogen X	C	H	X^-	N	C	H	Halide	N
		Diamine, mol/ml	CH_3I, mol/ml													
2	2	0.100/100	0.220/100	120	94.5	4.9	Methanol	I	24.02	5.54	63.44	7.00	24.16	5.47	63.27	6.97
3	2	0.100/100	0.220/100	120	0	99.6	95% ethanol	I	26.10	5.84	61.29	6.76	26.23	5.87	61.36	6.72
4	2	0.100/100	0.220/100	120	71.4	28.6	95% ethanol	I	28.05	6.12	59.28	6.54	27.94	6.16	59.20	6.41
		$N(CH_3)_3$, mol	Dibromide/CH_3OH, mol/ml													
5	3	0.252	0.100/150	260	0	99.2	93% ethanol	Br	37.95	8.11	45.90	8.05	38.03	8.14	45.90	7.99
8	3	0.244	0.100/200	360	0	99.9	Abs ethanol	Br	43.09	8.78	40.95	7.18	43.11	8.69	40.95	7.14
10	3	0.249	0.100/200 + 30Bz[c]	260	0	113.3	Abs ethanol	Br	45.95	9.16	38.21	6.70	45.86	9.14	38.08	6.68
16	3	0.0450	0.0150/40 + 40Bz	480	0	92.6	*n*-butanol	Br	52.59	10.03	31.81	5.58	52.44	10.08	31.85	5.50

[a] I: product filtered off from the mixture at the end of the reaction.
[b] II: product isolated from the mother liquor.
[c] Bz: benzene.

Table 4. Synthesis of the complexes with TCNQ anions from polymethylene *bis*-(trimethylammonium halides)[a]

Methonium		Compound, mmol	LiTCNQ, mmol	CH_3OH,[b] ml	Temperature, °C	Yield, %	Elemental composition						
							Calculated, %			Found, %			
n	Halogen						C	H	N	C	H	N	Halogen
2	I	1.00	2.00	50	RT	97.4							
		1.50	3.00	50	55–60	93.3							
		1.50	3.00	50	60–65	90.6	69.29	5.45	25.25	67.16	5.48	24.94	
3	I	1.50	3.00	50	40–50	76.2	69.70	5.67	24.63	69.32	5.71	24.89	
		1.50	3.00	50	40–50	84.3							
		1.50	3.00	100	60–65	79.9							
4	I	0.75	1.50	50	60–65	80.5							
		1.50	3.00	50	40–50	77.2	70.08	5.88	24.04	70.31	5.83	24.08	
5	Br	0.75	1.50	50	60–65	71.9							
		1.50	3.00	50	40–50	74.0	70.45	6.08	23.47	70.36	6.04	23.68	
6	I	0.75	1.50	50	60–65	78.2				70.60	6.38	22.70	Trace (I)
		1.50	3.00	50	40–50	83.3	70.80	6.27	22.93	70.94	6.20	22.88	
8	Br	0.75	1.50	50	60–65	84.7							
		1.50	3.00	50	40–50	91.5	71.45	6.63	21.93	71.64	6.55	21.92	
10	Br	0.75	1.50	50	60–65	82.7				72.02	7.10	20.68	Trace (Br)
		1.50	3.00	50	40–50	93.4	72.04	6.95	21.00	72.04	6.95	21.03	
16	Br	0.50	1.00	25	RT	91.3							
		0.50	1.00	25	40–50	88.0	73.57	7.78	18.65	73.43	7.80	18.58	
		0.75	1.50	50	60–65	79.3							

[a]The reactions were carried out at room temperature (RT: ~22°C) for 1.5 h. The reactions at elevated temperatures were carried out for 20 min and left at room temperature for 20 h before filtration.
[b]Amount of methanol used to dissolve each reactant.

Table 5. Electrical properties of the TCNQ complexes derived from polymethylene bis-(trimethylammonium halides)

Number of CH_2 Group (n)	With negative TCNQ			With negative and neutral TCNQ		
	ρ, Ω-cm	ϵ, eV	α, mV/°C	ρ, Ω-cm	ϵ, eV	α, mV/°C
2	1.9×10^3	0.12	+0.12	9.0×10^1	0.10	+0.043
3	1.3×10^5	0.24	+0.59	4.2×10^2	0.16	−0.060
4	3.1×10^7	0.41	+0.52	6.5×10^2	0.26	+0.132
5	4.0×10^6	0.29	+0.41	1.2×10^2	0.22	−0.150
6	5.0×10^{10}	0.73	Positive[a]	1.0×10^2	0.21	−0.143
8	3.7×10^7	0.41	+0.72	7.0×10^0	0.090	−0.010
10	3.6×10^7	0.44	+0.69	4.1×10^5	0.28	+0.64
16	1.4×10^9	0.46	+0.75	1.5×10^2	0.16	0

[a]The Seebeck coefficient was positive but its exact value could not be determined because of high impedance.

15 hours while the parallel solid line represents the resistivity of salts prepared at room temperature and allowed to crystallize for 3 days. In both cases the same relation between resistivity and the number of CH_2 groups was found.

The model compounds exhibited large variation in electrical properties. For the first series with TCNQ anions, only the specific resistivity varied in a broad range, reaching the maximum of 5×10^{10} Ω-cm for the salt with 6 methylene groups. The positive Seebeck coefficient exhibited by the polymeric salts indicates hole-type conductivity probably due to the electrically active lattice defects.

For the second series of complexes with neutral TCNQ, the magnitude of resistivity substantially decreased, especially where negative Seebeck coefficient was observed, indicating appearance of electron conductivity. The same relation between the negative Seebeck coefficient, electron conductivity, low resistivity, and low activation energy of conductivity was observed for polymeric complexes (Table 2 and Fig. 1).

c. Spectral properties. The spectra of all salts containing $TCNQ^-$ only exhibited two typical major bands at 4200 and 8420 Å. The intensity ratio of the two bands (~0.57) was independent of the number of CH_2 groups. The salts containing $TCNQ^0$ exhibited a λ_{max} at 3950 Å due to the neutral TCNQ molecule. The intensity ratio of the peak values at λ_{max} 3950 Å to that at λ_{max} 8420 Å varied from 0.9 to 1.6, the highest value representing the most conducting salt (with 8 CH_2 groups).

d. X-ray analysis. The materials investigated by single-crystal x-ray diffraction methods were TCNQ salts of model compounds of the following composition:

$[(CH_3)_3N^+(CH_2)_5N^+(CH_3)_3]$	$2(TCNQ^-)(TCNQ^0)$	I
$[(CH_3)_3N^+(CH_2)_5N^+(CH_3)_3]$	$2(TCNQ^-)$	II
$[(CH_3)_3N^+(CH_2)_6N^+(CH_3)_3]$	$2(TCNQ^-)(TCNQ^0)$	III
$[(CH_3)_3N^+(CH_2)_6N^+(CH_3)_3]$	$2(TCNQ^-)$	IV

Other crystals, listed in Table 5, were twinned and were too small to yield satisfactory diffraction patterns. I and IV yielded the most distinct and intense patterns. These two salts were found to have triclinic unit cells (Table 6). The dimensions of the unit cell of IV were substantially smaller than those of I, evidently due to the effect of two extra TCNQ molecules in the unit cell.

Table 6. Crystal structure

I. Model compound with 6 CH_2 groups and negative TCNQ.

Unit cell: Triclinic

$a = 11.500$ Å	$\alpha = 93°33'$
$b = 11.690$ Å	$\beta = 125°17'$
$c = 7.675$ Å	$\gamma = 95°40'$

$V = 829.53$ Å^3

II. Model compound with 5 CH_2 groups and negative and neutral TCNQ.

Unit cell: Triclinic

$a = 14.151$ Å	$\alpha = 98°29'$
$b = 7.829$ Å	$\beta = 108°07'$
$c = 13.813$ Å	$\gamma = 72°28'$

$V = 1384.39$ Å^3

Two other salts, II and III, gave less satisfactory diffraction patterns, which indicated nevertheless one-dimensional structures.

The unit cell parameters of I are recorded in Table 6. The (h o l) precession photograph showed a strong series of spots in the ($\bar{1}$ 0 4) direction (i.e., spots $\bar{1}$ 0 4, $\bar{2}$ 0 8, $\bar{3}$ 0 12 were very intense). This could be interpreted as stacking of electron density regions roughly perpendicular to the axis and separated by a repeat distance of 3.21 Å.

Salt II also showed evidence of 3.21 Å stacking as in salt I, but unfortunately crystal disorder effects prevented determination of unit cell dimensions.

As in the previous case, salt III showed a one-dimensional stacking effect (this time with a repeat distance of 3.11 Å), but further analysis was hampered by crystal twinning.

Salt IV gave very good diffraction patterns, but no evidence of any stacking phenomena was observed (i.e., no intense series of spots could be found in the diffraction pattern). The unit cell parameters are shown in Table 6.

3. Discussion

The values of ρ, ϵ, and α have been found to be reproducible within 30%. Further confidence in the accuracy of the results was gained by the use of disalts or polysalts synthesized under different experimental conditions, i.e., varying the temperature or solvent system. Essentially the same results were obtained indicating that the trends depicted in Figs. 1 and 2 are correct. The high values of

specific resistivities of 6-6 ionene polymers were independent of molecular weight (samples of approximate weight average molecular weight of 10,000, 25,000, and 80,000 were tested). In addition, the properties of *x-y* ionenes were identical to those of *y-x* ionenes.

In general, the examination of Figs. 1 and 2 and Tables 1, 2, 3, and 4 lead to the following conclusions:

(1) The highest specific resistivity and activation energy were observed for salts derived from model compounds or polymers containing 6 CH_2 groups.

(2) The salts with both negative and neutral TCNQ derived from the model compounds with 16 CH_2 groups and 6-16 ionene bromide exhibited very low specific resistivities, in spite of the fact that they contain the longest methylene chain between positive nitrogen atoms.

(3) The salts from the model compounds and the polymers with high specific resistivities invariably exhibited hole-type conductivity or positive Seebeck coefficients, while those with low specific resistivities were characterized by electron-type conductivity or negative Seebeck coefficients.

(4) The salts with 16 CH_2 groups exhibited low Seebeck coefficients. The lowest concentrations of the charge in these salts gave rise to a mixed-type conductivity with the same concentration of holes and electrons.

(5) The characteristic variations of specific resistivity as a function of the number of CH_2 groups can be attributed to the conformations of polymethylene chains in the solid state, the high conductivity being due to electron delocalization in one-dimensional TCNQ columns.

The resistivity value of the polysalt containing 6 CH_2 groups between positive nitrogens and only $TCNQ^-$ is also highest in the analogous model salts (Fig. 2). The fact that TCNQ salt of the model compound (salt IV, see *Subsection d*) exhibits a resistivity value of the order of 10^2 Ω-cm seems to be out of line. It can be understood on the basis of the x-ray investigations. The geometry of the salts formed is the dominant factor in the electrical values of the materials under investigation and it is only when one-dimensional column stacking of the TCNQ moiety occurs that a very high electronic conductivity is observed. It is therefore not surprising to note that a decrease of concentration of positive charges in the polymeric chain or in the model compounds does not necessarily increase the values of ρ or ϵ (Figs. 1 and 2).

The preliminary x-ray data support the anomalously high resistivity of salt IV as compared with salt II. Salts I and II have even lower resistivities and lower activation energy of conductivity. This is consistent with the x-ray results, for salt IV is the only one of the four compounds studied which shows no evidence of one-dimensional stacking.

References

1. Melby, L. R., et al., *J. Am. Chem. Soc.*, Vol. 84, p. 3374, 1962.
2. Rembaum, A., et al., *J. Phys. Chem.*, Vol. 73, p. 513, 1969.
3. Rembaum, A., *J. Polym. Sci.*, Part C, No. 29, p. 157, 1970.
4. Kepler, R. G., *Phonons and Phonons Interactions*, p. 579. Edited by T. A. Bak. W. A. Benjamin, Inc., New York, 1964.
5. Rembaum, A., Baumgartner, W., and Eisenberg, A., *J. Polym. Sci.*, Part B, No. 6, p. 169, 1968.
6. Rembaum, A., Rile, H., and Somoano, R., *J. Poly Sci.*, Part B, p. 457, 1970.

D. Evaluation of Magnetic Recording Tapes: A Method for the Quantitative Determination of Stick–Slip, *R. H. Silver, S. H. Kalfayan, and J. K. Hoffman*[1]

1. Introduction

The behavior known as "stick–slip," encountered with magnetic recording tapes, was discussed previously (SPS 37-63, -64, and -65, Vol. III). The quantitative determination of this phenomenon, that is, the measuring of the degree or extent of stick–slip, under different conditions would be most desirable. This article discusses a method developed to achieve this end *without using a tape transport.*

2. Discussion

Stick–slip will cause a variation in the tape-to-head speed. Sticking will decrease and slipping will increase the speed of the tape passing over the magnetic heads.

[1]Spacecraft Data Systems Section, Astrionics Division.

If the instantaneous speed of the tape could be determined, then this would serve as a measure of the degree of stick and slip.

Instead of attempting the very difficult direct measurement of the instantaneous speed of the tape, we have measured a factor which is a manifestation of the change in speed. This factor is the apparent period of a cycle in the signal recorded on the tape. The explanation is as follows.

A sinusoidal electrical signal is recorded[2] on a portion of magnetic tape to be evaluated. The tape is then mounted, along with the heads in the Instron test apparatus, in the same manner as described previously (SPS 37-63, Vol. III, pp. 209–214), and as shown in Fig. 1. Electrical connections are then made to the pickup coil of the magnetic head, which is connected to an amplifier.[3] The signal therefrom is fed into a digital period counter and a paper tape printout.[4] The cycle period, in seconds, of the recorded signal can be measured accurately by oscilloscopic examination of the tape during initial recording.

If the speed of the tape passing over the heads remains constant, then the period of the recorded electrical signal will also be constant. If, however, the speed of the tape should vary because of sticking and slipping, the apparent period of the recorded signal will also vary. The extent of the variation of the period from its original value (the standard deviation σ) will be a measure of the degree of stick–slip.

3. Experimental Procedures and Results

A length of new CEC-W4 magnetic recording tape was prerecorded with a 9000 ±30-Hz signal at 15-in./s speed, and at saturation voltage. The tape was then placed in the Instron test apparatus at ambient temperature and humidity, and passed over 2 brass heads for a total of 40 passes at a crosshead speed of 0.166 in./s. During each pass both the force experienced by the load cell and the period of every tenth cycle of the electrical signal were recorded. There were approximately 75 cycle periods recorded for each pass, a pass being the downward journey of the 110-g weight pulling the tape over the magnetic heads.

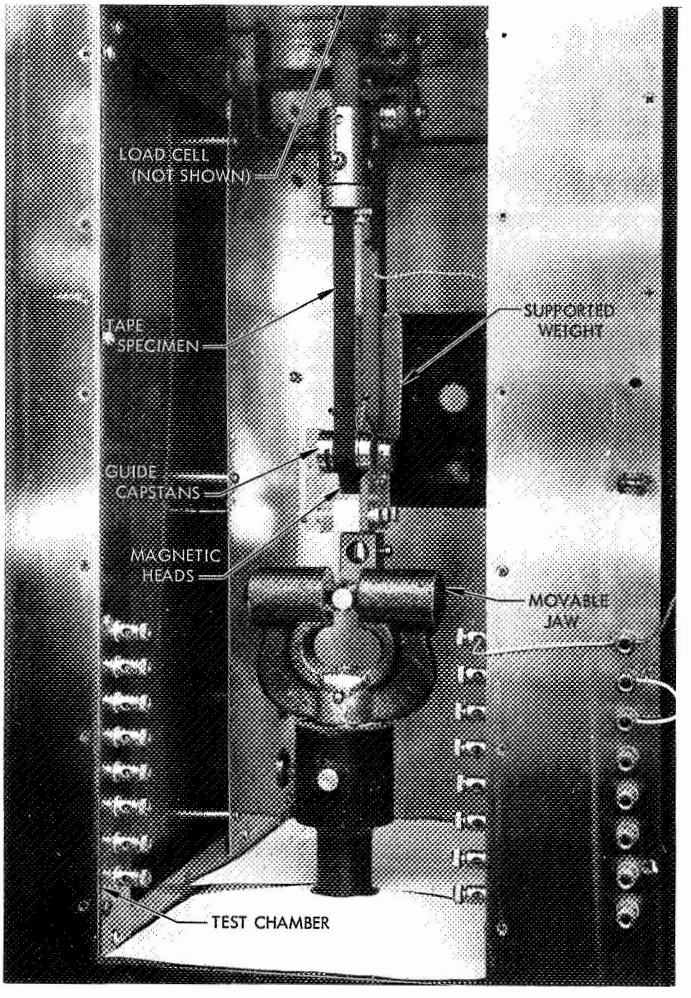

Fig. 1. Test apparatus

Frequency f is inversely proportional to period π:

$$f = \frac{1}{\pi} \tag{1}$$

The following relationships are assumed to hold true and should yield the standard deviation for speed:

$$\frac{f}{\sigma_f} = \frac{S_{CH}}{\sigma_s}$$

or because of Eq. (1):

$$\frac{\sigma_\pi}{\pi} = \frac{S_{CH}}{\sigma_s}$$

[2]Model 651B test oscillator (Hewlett-Packard)/Ampex Model FR-100 magnetic tape test recorder.

[3]Astrodata Model 120 nanovolt amplifier.

[4]Model 5532A electronic counter (Hewlett-Packard)/Model H43562Z digital recorder (Hewlett-Packard).

or

$$\sigma_s = \frac{S_{CH} \times \pi}{\sigma_\pi} \tag{2}$$

where

σ_f = standard deviation of frequency values

S_{CH} = crosshead speed

σ_π = standard deviation of period values

σ_s = standard deviation of speed values

The crosshead speed S_{CH} was held constant at 0.166 in./s and the average period was found to be 0.0100 seconds, which agreed well with the calculated value of 0.01002 seconds, obtained from the known frequency and speed:

$$f = \frac{\text{Recorded frequency (Hz)} \times \text{Crosshead speed (in./s)}}{\text{Speed of tape at recording (in./s)}}$$

$$= \frac{9 \times 10^3 \text{ Hz} \times 0.166 \text{ in./s}}{15 \text{ in./s}} = 99.6 \text{ Hz}$$

Since

$$\pi = \frac{1}{f}$$

$$\pi = \frac{1}{99.6} = 0.01002 \text{ seconds}$$

The σ_π was computed from the test data, and, therefore, σ_s could be calculated from Eq. (2).

The plot of log σ_s versus the number of passes (Fig. 2) indicates how severely the standard deviation changes; therefore the stick–slip increases by the repeated passage of this tape over the magnetic heads. It must be kept in mind, however, that the worst conditions were selected for this experiment, in order to point out the measurability of stick–slip from apparent changes in the cycle period. *The conditions used were different from those customarily associated with spacecraft tape recorder applications.* Experiments are in progress to determine σ_s for tapes under normal use conditions.

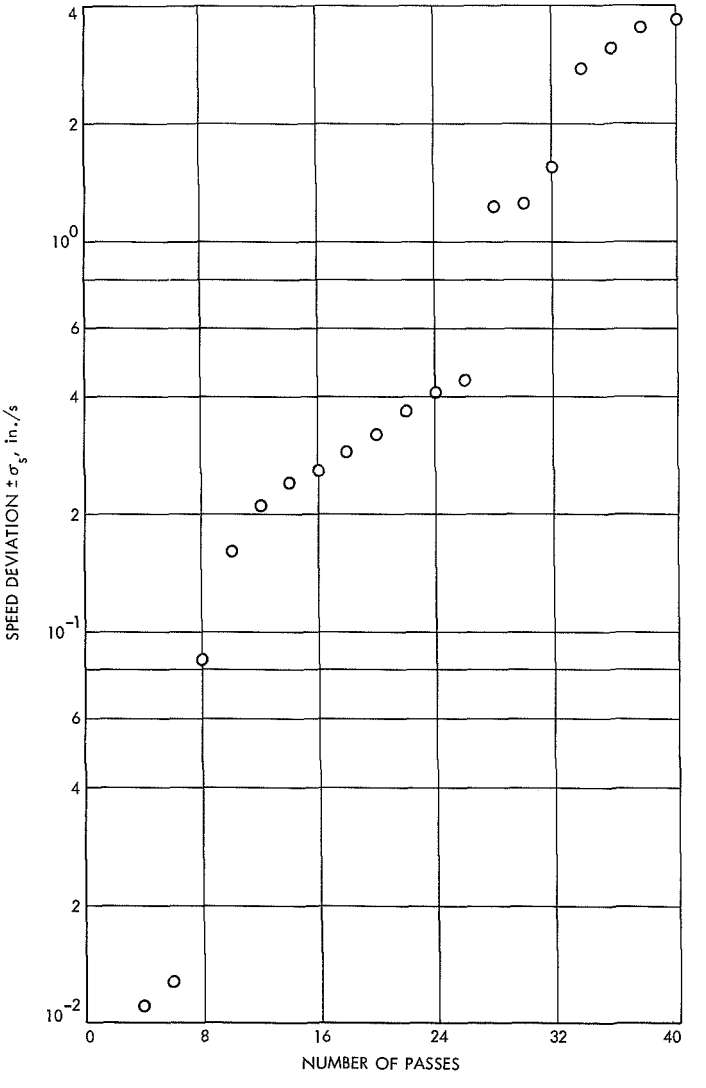

Fig. 2. Speed deviation vs number of passes